PROBLEMY MECHATRONIKI
UZBROJENIE, LOTNICTWO, INŻYNIERIA BEZPIECZEŃSTWA

ISSN 2081-5891

8, 1 (27), 2017, 115-128

PROBLEMS OF MECHATRONICS
ARMAMENT, AVIATION, SAFETY ENGINEERING

Investigating a Process of Accelerating Macroscopic Objects in an Eddy-Current Inductance Coil Magnetic Field

Andrzej HORODEŃSKI*, Cezary POCHRYBNIAK, Kamil NAMYŚLAK

National Centre for Nuclear Research
7 Andrzeja Sołtana Street, 05-400 Otwock, Poland
**Corresponding author's email address: Andrzej.Horodenski@ncbj.gov.pl*

Received by the editorial staff on 14 June 2016.
The reviewed and verified version was received on 27 December 2016.

DOI 10.5604/01.3001.0009.8998

Abstract. The subject of this paper is an analysis of the process of applying kinetic energy to a projectile made of non-magnetic electrically conductive material and located inside an induction coil live with alternating current. An experimental verification was carried out of the analytical conclusions that were pertinent to the design and technology of an inductance coil gun, which is a ranged weapon type.
Keywords: mechanics, coil gun, acceleration, electromagnetic force, coil, propulsion, electromagnetism

This work has been compiled from the paper presented during the 11th International Armament Conference on Scientific Aspects of Armament and Safety Technology, Ryn, Poland, 19 to 22 September 2016

1. INTRODUCTION

The subject of this paper is an analysis of the process of applying kinetic energy to a projectile made of non-magnetic electrically conductive material and located inside an induction coil live with alternating current, and a preliminary verification of the conclusion of this analysis. ICG ranged weapons (which do not employ explosive or combustion propellants) are currently the focus of study of many laboratories around the world [1-2].

In an ICG system which comprises a projectile with a coil, the axial component of the magnetic field generates a circulating eddy current which acts on the radial component of the same magnetic field and propels the projectile to translate it.

The energy input to affect the shot of this projectile has 8 outputs:

1. generation of velocity of the projectile by the effect of the magnetic field radial component on the current induced in the projectile;
2. generation of torque of the projectile by the effect of the magnetic field azimuthal component on the current induced in the projectile (and this effect is negligible in the ICG configurations used at the current stage of research);
3. compression of the projectile by the effect of the magnetic field axial component on the current induced in the projectile;
4. generation of oscillation of the inductance coil by the effect of the coil magnetic field on the coil current;
5. resistive heating of the projectile material;
6. loss of the power supply system;
7. exchange of momentum with the accelerating coil mass;
8. electromagnetic wave emission (from 5 to 10 kHz), which is negligible with the frequencies and geometrical dimensions of the ICG in question.

The design of the ICG and the technologies applied thereto must ensure optimisation of process 1 (and process 2, potentially) while minimizing the effects of processes 3 to 8.

Examples of calculations were carried out for a projectile made of Duralumin and sized as follows: coil outer diameter d_z = 35 mm, coil inner diameter d_w = 30 mm. Working assumptions were made as follows: coil length l = 6 cm, number of coil turns n = 30, coil inductance L = 40 μH (which was much higher than the series inductance of the power supply unit), energy bank capacity C = 25 μF, charging U_0 = 10 kV (providing a peak current of ca. I_0 = 7.7 kA, and stored energy E_0 = 1200 J).

2. MAGNETIC FIELD

The distribution of the magnetic fields and forces applied to the projectile was expressed as follows (with cylindrical coordinates):

$$\mathbf{B} = [B_r, B_\varphi, B_z],$$

$$\mathbf{I} = [0, I_\varphi, I_z].$$

Coupling the magnetic field with the eddy current resulted in a Lorentz force that acted on the projectile as follows:

$$\mathbf{F} = \mathbf{I} \times \mathbf{B}$$

with a variety of components:

$F_z = B_r * I_\varphi$ – projectile acceleration,
$F_r = B_z * I_\varphi$ – projectile compression,
$F_\varphi = B_r * I_z$ – torque generation.

The focus of subsequent calculations was solely the radial component of the magnetic field (as required to calculate the accelerating force) and the axial component (resulting in projectile compression) of the magnetic field.

It was possible to calculate the distribution of the radial and axial components of the magnetic field at a preset distance from the inductance coil axis with a relatively high accuracy by using the formulas [4, 5]:

$$h_r(z,r) = \frac{1}{2a}\int_{-a}^{a} \frac{(z-u)\left(\left(r^2+(z-u)^2+1\right)E\left(-\frac{4r}{(r-1)^2+(z-u)^2}\right)-\left((r+1)^2+(z-u)^2\right)K\left(-\frac{4r}{(r-1)^2+(z-u)^2}\right)\right)}{2\pi r\sqrt{(r-1)^2+(z-u)^2}\left((r+1)^2+(z-u)^2\right)}\,du$$

$$h_z(z,r) = \frac{1}{2a}\int_{-a}^{a} \frac{\left((r+1)^2+(z-u)^2\right)K\left(-\frac{4r}{(r-1)^2+(z-u)^2}\right)-\left(r^2+(z-u)^2-1\right)E\left(-\frac{4r}{(r-1)^2+(z-u)^2}\right)}{2\pi\sqrt{(r-1)^2+(z-u)^2}\left((r+1)^2+(z-u)^2\right)}\,du$$

with: E and K – elliptical integrals, and r and z – cylindrical coordinates relative to the coil radius R, and a – half length of the coil, and: $h = H/H_{odn}$, $H_{odn} = i/R$, where i denotes the coil current.

Figure 1 shows an example of the distribution calculated for the magnetic field radial and axial components.

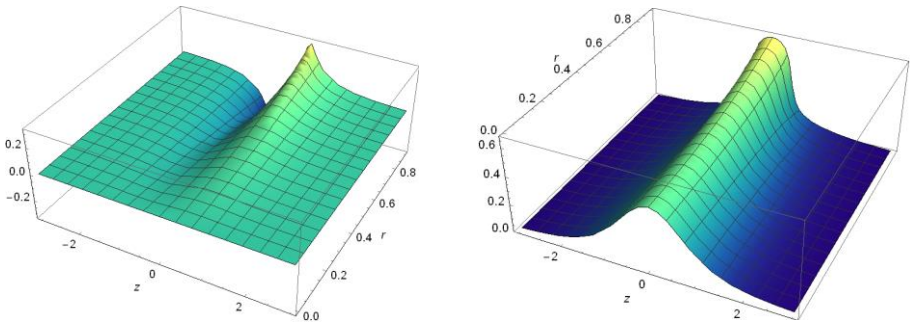

Fig. 1. Examples of distribution of the magnetic field (a) radial and (b) axial components along the inductance coil radius in various axial positions

The values of the magnetic field radial and axial components and the value of the electrodynamic force they generated at various axial positions at a distance from the projectile and coil system axis of symmetry equal to 0.9 of radius are shown in Fig. 2

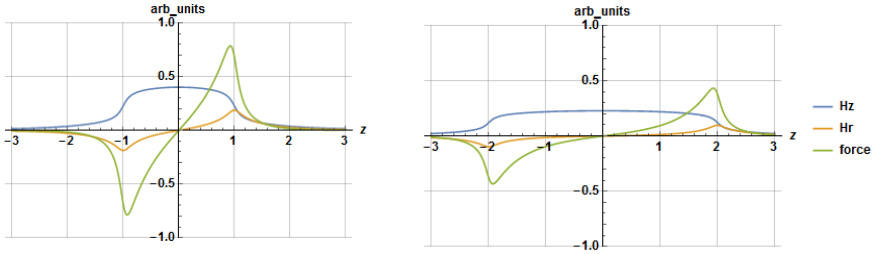

Fig. 2. Relative values of the magnetic field radial and axial components and the electrodynamic force for: (a) a short inductance coil (L/D = 1) and (b) long inductance coil (L/D = 2) at a radial position r = 0.9 (within the area of induced eddy current)

3. ELECTRIC CIRCUIT

The projectile and coil system was a system of coupled inductance that was powered with current from a capacitance bank, see Fig. 3.

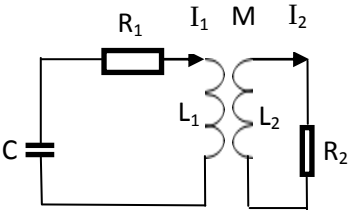

Fig. 3. RLCM system

Here, the secondary circuit was represented by the eddy current generated within the projectile material and flowing along the projectile circumference. The operation of this system, designated RLCM, is defined by a set of equations:

$$1/C \int I_1\,dt + L_1\,dI_1/dt + R_1\,I_1 + M\,dI_2/dt = 0$$

$$M\,dI_1/dt + L_2\,dI_2/dt + R_2 I_2 = 0$$

with:

C – energy bank capacity,

R_1, R_2 – primary and secondary side resistance, respectively,

M – mutual inductance,

L_1, L_2 – primary and secondary side inductance, respectively.

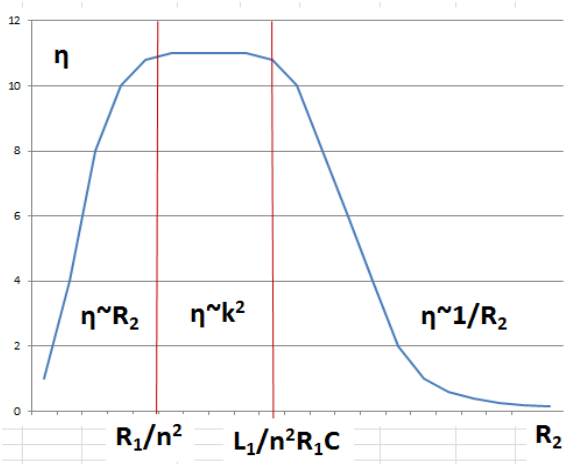

Fig. 4. Energy efficiency of the RLCM system vs. load resistance

The energy efficiency of the RLCM system, expressed as the ratio of the energy emitted as secondary resistance to the capacitor energy is shown in Fig. 4 [3]. It is evident that an interval in which the energy efficiency would achieve its maximum value, contained largely by the coupling coefficient, had the following condition to meet:

$$R_1/n^2 < L_1/n^2 R_1 C$$

which can be reduced as follows: $R_1 < \sqrt{(L_1/C)}$

The power supply systems investigated herein met the condition satisfactorily: $R_1 \approx 50 - 300$ mΩ, $\sqrt{(L_1/C)} \approx 1$ Ω, whereas the investigated ICG was operated in a range of $R_2 < R_1/n^2$ (see Fig. 3, left side of the plot). Under these conditions, the inequality as follows was properly met:

$$\alpha << \omega$$

which means that the discharge current was an expiring oscillation.

As demonstrated in [3], the power supply system performance and parameters can be expressed in the following relationships:

$$I_1(t) = I_0 \exp(-\alpha t) \sin(\omega t) \quad (1)$$

$$I_2 = n\, k\, I_1 \quad (2)$$

with:

$n = \sqrt{(L_1 / L_2)}$ – number of coil turns (approximate),

k – projectile to coil coupling coefficient,

what follows is:

$I_0 = U_0\sqrt{(C/L)}$, $\alpha = R/2L$, $R = R_1 + k^2 n^2 R_2$, $\omega = 1/\sqrt{(LC)}$, $L = (1 - k^2)\, L_1$

The coupling coefficient can be estimated with a good accuracy as a ratio of the projectile cross-sectional area to the coil mean cross-sectional area:

$$k = (d_{proj}/d_{coil\_mean})^2$$

These findings allowed a relatively easy analysis of the system performance by analysing the resistance values present therein as introduced by the specific energy outputs.

The resistance of the electric circuit comprised:

- on the primary side:
  - ✓ power bank internal resistance,
  - ✓ resistance of energy dissipation by the natural vibration of the coil,
  - ✓ resistance of the coil wire and system connection leads;
- on the secondary side:
  - ✓ material resistivity, generating the projectile material temperature increase,
  - ✓ resistance of the energy output for the projectile compression,
  - ✓ resistance of the kinetic energy generation in the projectile.

4. PROJECTILE ACCELERATION

The radial component of the magnetic induction generated by the inductance coil was approximately equal to:

$$B_r = \mu_o\, n\, h_r\, I_1 / l \quad (3)$$

with:

I_1 – primary circuit current,

$\mu_o = 4\pi*10^{-7}$ H/m – magnetic permeability of vacuum,

n – number of coil turns, or the projectile to coil transformation ratio,

l – coil length,

h_r – maximum relative value of the magnetic field radial component.

The force which acted on the projectile on the surface of which the current I_2 was flowing can be estimated with a Lorentz formula:

$$F_z = \pi\, h_z\, \mathrm{d}\, I_2\, B_r \tag{4}$$

with:

d – coil inner diameter,

h_z – maximum relative value of the magnetic field axial component.

The formulas (3) and (4) show what follows:

$$F_z = \pi\, \mu_o\, h_r\, d\, n\, /l * I_1\, I_2$$

Concerning the relationship (2), the time distribution of the electrodynamic force can be expressed as follows:

$$F_z\,(\mathrm{t}) = \pi\, \mu_o\, h_r\, h_z\, d\, k_{ef}\, n^2\, /l * I_1^2(t)$$

with the current I_1 expressed with the formula (1).

Given the following:

$$L_1 = \pi\, \mu_o\, d^2\, n^2\, /4l$$

the following is produced:

$$F_z\,(t) = F_0{*}\exp(-2\alpha t)\, \sin(\omega t) \tag{5}$$

with: $F_0 = 8\, k_{ef}\, h_r\, h_z\, E_0/d$

An example of the value of the electrodynamic force which accelerated the projectile is ca. $F_0 \approx 40$ kN at a power supply energy input of $E_0 = 1200$ J.

The kinetic energy of the projectile located inside the live inductance coil was generated with the Lorentz force, which in turn was generated by the effect of the magnetic field radial component on the eddy current induced within the projectile itself that was made of a non-magnetic conductive material. The generated momentum of the projectile was calculated with an equation of momentum and impulse:

$$\int F_z\, \mathrm{d}t = m\, v_{proj}$$

Hence:

$$v = 8\, k_{ef} E_0/md \int_0^{\infty} \exp(-2\alpha t)\, \sin^2(\omega t)\, \mathrm{d}t \approx \frac{4\, h_r\, h_z\, k_{ef}\, \chi\, E_0}{m\, d\, \alpha}$$

with: χ – the energy partition coefficient imposed by the balance of moments (see section 5.1)

This implies that the muzzle velocity of the projectile was directly proportional to the energy stored in the capacitor bank, whereas the energy efficiency of the projectile acceleration process was increasing with the power supply energy input:

$$\eta \approx \frac{8 h_r^2\, h_z^2\, k_{ef}^2\, \chi^2\, E_0}{m\, d^2\, \alpha^2} \tag{6}$$

5. ENERGY LOSS

5.1. Balance of moments

The projectile and coil system was a specific case of two massive bodies, with one of them (the coil) acting on the other (the projectile) according to the momentum conservation. When the inductance coil pushed out the projectile from the magnetic force effect area, it applied momentum both to the projectile and itself, and the sum of momentums was equal to zero. Hence the projectile energy share of the total projectile and coil system energy:

$$\chi = E_{proj}/E_{total} = 1/(1+\zeta),$$

with: $\zeta = m_{proj}/m_{coil}$

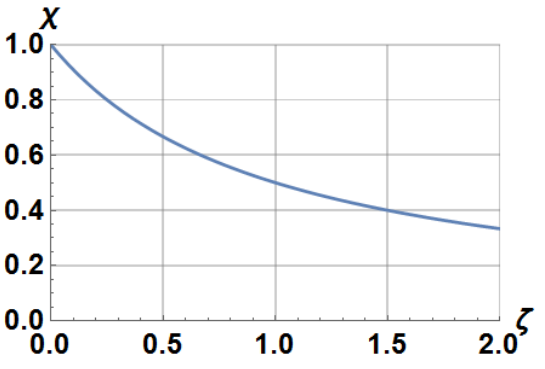

Fig. 5. Share of the projectile energy in the total system energy from the balance of momentums

The projectile and the coil shared the energy inversely to the ratio of their masses. This was significant to the technology of the inductance coil. First, a coil made of thick wire with the maximum viable wire size (cross-sectional area) should be used. Second, it is necessary to firmly anchor the coil to its body so that the two parts become the repulsive mass.

5.2. Coil natural vibration

The coil is mechanically excited by the current oscillated with a frequency of the current alternation; hence the voltage drop across the coil can be expressed as follows:

$$U = d/\mathrm{d}t(L*I) = L* \mathrm{d}I/\mathrm{d}t + I* \mathrm{d}L/\mathrm{d}t$$

The second component of this equation is resistance:

$$\mathrm{d}L/\mathrm{d}t = \mathrm{d}L/\mathrm{d}I*\mathrm{d}I/\mathrm{d}t = R_{\mathrm{vib}}$$

Given that the coil wire material deformation did not exceed the elastic limit, the vibration value was proportional to the actual current value:

$$\mathrm{d}L/\mathrm{d}I = \beta*I$$

with: β – constant of proportionality.

The relationships are:

$$R_{\mathrm{vib}} = \omega\, \beta\, I_0^2 \exp(-2\alpha t)\sin(\omega t)\cos(\omega t)$$

the time-averaged value of which is:

$$<R_{\mathrm{vib}}> \approx \alpha\, \beta\, I_0^2 \int_0^{\infty} \exp(-2\alpha t)\sin(\omega t)\cos(\omega t)\mathrm{d}(\omega t) \approx \beta\, I_0^2/4 = \alpha\, \Delta L\, /4$$

The laws of electrodynamics state that the coil vibrates in two directions, axial and radial. The axial vibration of a solenoid coil is caused by the forces of mutual attraction between the adjacent coil turns, whereas the radial vibration of the same coil type is caused by repulsion of the coil parts that are located opposite to each other. Given the extremely small distance between the adjacent coil turns, the axial vibrations are predominant. A layered coil should be expected to feature predominantly radial vibrations.

Given a current surge with a peak of I_0 = 1 kA and a space for the coil diameter variations of ca. 0.1 mm, i.e. an inductance increase of ΔL and equal to ca. 0.1 μH, the resistance input to the circuit can be estimated at ca. 25-50 mΩ, depending on the number of coil turns. The input of axial vibrations to the resistance of loss can be critical to the energy input from the capacitive buffer to the projectile.

Additional input came from the non-elastic deformation of the coil and body materials subject to deformation from intense vibration.

These findings must be considered when designing the structure and operating technology of an ICG coil.

5.3. Projectile compression

The magnetic field axial component reacted with the induced current and caused compression of the projectile material:

$$F_r = B_z * I_\varphi = -\gamma\, \Delta r$$

with: γ – coefficient of elasticity

The energy consumption during this compression process depends on whether the projectile material compression, as caused by the electromagnetic force radial component, remains within the elastic range or moves to the plastic range. If the deformation value is confined within the elastic range, the momentum thus transferred is returned to the system without any apparent losses.

The formula (5) gives the peak compressive pressure value acting on the projectile surface:

$$\varrho = F_0 / S_{proj} = 8k_{ef} E_0/(\pi d^2 l)$$

with: S_{proj} – projectile lateral surface.

An example of this value at $U = 20$ kV, $C = 25$ μF was $\varrho \approx 80$ MPa. This value is comparable to the yield strength of a large number of metals and alloys.

5.4. Projectile heating

According to the Ohm's law, the eddy current induced in the projectile caused a release of heat and increased the surface layer temperature of the projectile. The resistance of the conductive layer depends on the resistivity of the projectile material and the base frequency of the current. In the case contemplated herein (with the material being Duralumin PA6 and a frequency of 5-10 kHz), an assumption can be made that the current layer thickness was ca. 1 mm with a secondary ohmic resistance at $R_{2heat} = 0.03$ mΩ.
The same resistance was as follows in the primary circuit:

$$R_{heat} = k^2 n^2 R_{2heat}$$

resulting in a heat consumption equal to:

$$E_{heat} = \int_0^\infty I_1^2 R_{heat}\, dt = k^2 n^2 E_0 R_{heat}/4R_{circuit}$$

Hence the estimated losses on projectile heating were at least ten-odd percent, whereas the projectile temperature increase ranged from several to several dozen degrees, depending on the energy input, frequency and projectile material (see the examples of values: $R_{heat} \approx 0.5$ mΩ, $E_{heat} \approx 200$ J).

6. PROJECTILE WITH AN AXIAL FULL-LENGTH BORE

The induced current flowed within the projectile in a thin (1 mm) superficial current layer. Hence, a projectile with a full-length bore along the central axis can be used in the ICG. This configuration has several advantages to the design engineering and target application:

- the reduction of projectile weight does not change the energy consumption; it only increases the projectile velocity;
- the induced current flows both on the outer and the inner surfaces of the projectile, which improves the energy transfer;
- the velocity increase inside the accelerating duct is more effective because of a significant reduction of drag;
- a suitably modified inductance coil may spin the projectile for better in-flight stability; alternatively, stabilizer fins can be installed within the projectile bore.

The full-length bore projectile is now pending a patent from the Polish Patent Office.

7. MEASUREMENTS

The estimations presented herein were verified in two stages. The first stage involved verification with a measurement system, comprising a power supply energy input bank with a capacity of $C = 25$ μF, a self-inductance of 1.6 μH, and a series resistance of ca. 40 mΩ. This capacitor bank was charged to a voltage of 8-18 kV (i.e. an energy of 0.8-4 kJ). The second stage of verification included a similar measurement system with a capacity of $C = 12.5$ μF, a self-inductance of 0.33 μH, and a series resistance of 40 mΩ. This capacitor bank was charged to a voltage of 15-30 kV (i.e. an energy of 1.4-5.6 kJ). At both stages of verification, the power supply system was switched with a field distortion spark gap initiated by a starter that generated a low-energy voltage pulse peaking to 60 kV.

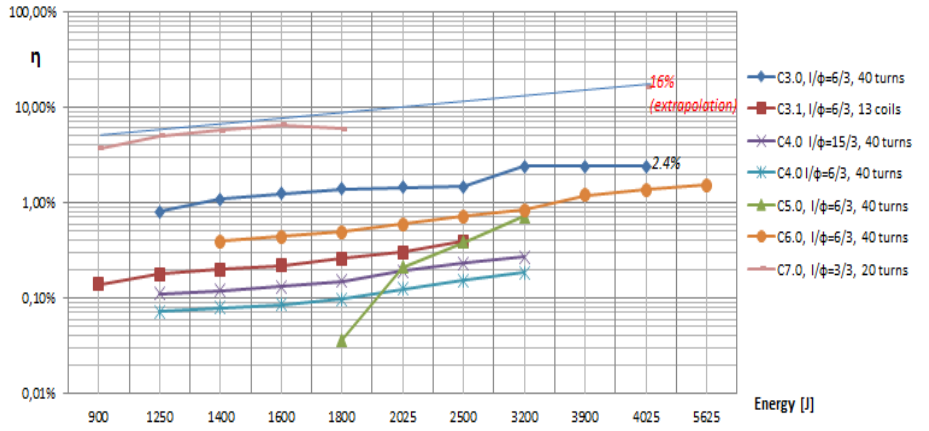

Fig. 6. Measurement results for the kinetic energy of various coil configurations and technologies vs. energy input

Tests were performed on the process of accelerating cylindrical projectiles made of Duralumin PA6, 4-6 cm long, 2-3 mm in wall thickness, and 28-35 g in weight, and propelled with a coil with a length from 3 cm to 15 cm, made of Cu wire with a cross-sectional width of 2 or 3 mm, and built as a single or three-layer solenoid with 12 to 15 turns per layer. The projectile velocity was measured with a system comprising a LED and a phototransistor which measured the projectile flight time over a distance of ca. 50 cm. This test system is shown in Image 1.

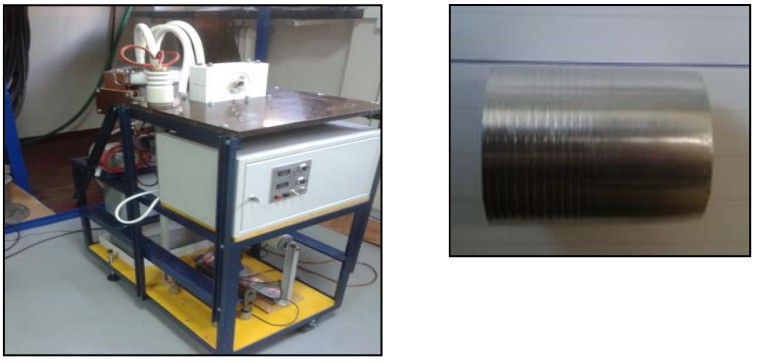

Image 1. Test system (see left) and an example of the test projectile (see right)

The aggregated measurement results of the system energy efficiency defined as the ratio of the projectile kinetic energy to the capacitor bank stored energy, and provided by both energy banks, are shown in Fig. 6.

8. CONCLUSIONS

The tests completed so far confirm that the initial evaluation of the power supply requirements, coil geometry, and processes of projectile acceleration were correct in general. The measurements confirmed virtually all analytical forecasts, both in qualitative and (partially) quantitative terms, including:

- the effects of the inductance coil form and dimensions (especially the length to O.D. ratio);
- the effect of coil vibration on the acceleration energy efficiency;
- the significance of the balance of momentums of the coil and the projectile;
- the importance of the power supply energy input bank parameters (and especially its series inductance);
- the exposure of the projectile to compression.

These findings allow formulating the technological and design requirements for future ICG (inductance coil guns).

The results provided by the coil version 7.0 (a short coil with a diameter and a length of 3 cm each) deserve an expanded commentary. This version, which had the technology most improved of all previous evolutions, generated a projectile velocity of 80 m/s and (what is more important), an energy-to-projectile transfer efficiency as high as 6.5%, with an energy input below 1,600 J. These parameter values greatly outranked any previous results.

Extrapolating these results to the previous energy levels of 4 kJ should provide an energy transfer efficiency of 16% and a projectile velocity of 180 m/s, or 300 m/s at 10 kJ. The development of an inductance coil with a supply energy of 20 kJ or more is a realistic prospect of building ICGs with a full potential for practical applications.

As expected, the greatest design engineering and technological problem is the resistance of the coil to high current surges and mechanical shocks. Another essential problem is an effective method of attenuating coil vibrations, which, if not controlled, reduce the overall energy efficiency of an ICG system. What is also of utmost importance is the resistance of the coil turn-to-turn insulation to strong mechanical shocks; the compression of this insulation system gradually increases the coil vibration gap.

The tests and research completed so far have included generally available materials, e.g. Novotex, Ertalon, Teflon, Epidian, etc. The reported research has proven that the performance of those materials as insulators is insufficient for building a target ICG. Materials of much better mechanical, insulating and thermal performance are required.

REFERENCES

[1] Fair Harry D. 2013. "The Past, Present, and Future of Electromagnetic Launch Technology", *IEEE Transactions On Plasma Science*, 41(5).
[2] Conference Proceedings of the 18th International Symposium on Electromagnetic Launch Technology, Wuhan, China, October 24-28, 2016.
[3] Horodeński Andrzej, *Impulsowe grzanie cienkich warstw metalu w układzie rozładowczym z obciążeniem transformatorowym*, IBJ Internal Report No. 0-148/XXIV/79.
[4] Horodeński Andrzej. 2016. *Optymalizacja kształtu cewki napędowej urządzenia miotającego typu Inductance Coil Gun,* NCBJ Internal Report.
[5] Wciślik Mirosław, Tomasz Kwaśniewski. 2006. „Model cylindrycznej cewki jednowarstwowej". *Przegląd Elektrotechniczny* 82 (11).

Badanie procesu akceleracji obiektów makroskopowych w polu magnetycznym cewki indukcyjnej z wykorzystaniem prądów wirowych

Andrzej HORODEŃSKI, Cezary POCHRYBNIAK,
Kamil NAMYŚLAK

Narodowe Centrum Badań Jądrowych
ul. Andrzeja Sołtana 7, 05-400 Otwock

Streszczenie. Przedmiotem pracy jest analiza procesu nadawania energii kinetycznej pociskowi wykonanemu z niemagnetycznego materiału przewodzącego, umieszczonemu wewnątrz cewki, przez którą płynie prąd zmienny. Dokonano eksperymentalnej weryfikacji płynących z analizy wniosków istotnych z punktu widzenia konstrukcji i technologii urządzenia miotającego typu Inductance Coil Gun (ICG).
Słowa kluczowe: mechanika, coilgun, cewka, miotanie, siła elektromagnetyczna